

---

---

# Selection Tool for Water-Resistive Barriers with Suitable Vapor Permeability

Marcus Jablonka

Achilles Karagiozis, PhD

John Straube, PhD  
Associate Member ASHRAE

## ABSTRACT

*Over the past several decades, advances in the application of polymers brought new polymeric water-resistive barriers with a wide range of vapor permeability to market, commonly referred to as “breathable” housewraps. However, at this time there is virtually no guidance available regarding the selection of the optimum vapor permeability of such membranes under specific conditions.*

*This paper evaluates the impact of various water-resistive barriers with a large range of vapor permeability on the hygro-thermal performance of different wall assemblies. The information enables designers to select products with the most suitable vapor permeability for particular geographical locations and construction conditions. Variations in boundary conditions included climatic conditions (seven climatic locations), cladding type (three-coat stucco, manufactured stone, cement board, brick), and type of WRB (low versus high vapor permeability) deployed. The results for the performance of the wall systems are presented in form of a mold index.*

---

## INTRODUCTION

The primary function of a water-resistive barrier (WRB) in a building enclosure system is to serve as a second line of defense and shed water that penetrates the cladding. Even though the building enclosure may be designed properly by design professionals, experience shows that defects created during the construction process or those occurring during the service life of the structure may allow water to enter the wall assembly. Hence, for a wall assembly to function well, it should be designed to permit drainage on the surface of the water-resistive barrier and—particularly important for wood frame construction—drying of any excess moisture. Therefore, the water-resistive barrier is required to be vapor permeable in order to allow for outward diffusion of water vapor. The moisture balance of the building material adjacent to the water-resistive barrier will be strongly affected by the water vapor flow caused by thermal drive, which may vary depending on the moisture content, temperature of outdoor air, and solar radiation. A reverse thermal gradient may cause inward

vapor diffusion into the wall cavity. For this reason water-resistive barriers need to be evaluated in regards to their effect on the performance of a wall assembly (Jablonka 2011).

Different types of water-resistive barriers may be incorporated into the wall assembly, and—depending on climatic conditions and the type of sheathing and cladding material used—may have different effects on its performance and durability. The available variety and characteristics of such membrane products have changed significantly over the past several decades. Advances in the application of polymers brought a large variety of “breathable” housewraps with a wide range of vapor permeability to market. However, the large variety of performance characteristics of such membrane products has resulted in uncertainty among design professionals and the construction industry at large regarding the in-service performance of various types of water-resistive barriers and the selection of the optimum vapor permeability under specific conditions. This paper describes a research project that evaluates the impact of various water-resistive

---

*Marcus Jablonka is director at Cosella-Dorken Products, Beamsville, ON, Canada. Achilles Karagiozis is a distinguished research engineer at Oak Ridge National Laboratory, Oak Ridge, TN, USA. John Straube is a principal at Building Science Consulting, Waterloo, ON, Canada.*

barriers with a large range of vapor permeability on the hygrothermal performance of different wall assemblies—information vitally important for proper product selection. For the convenience of designers the results of this research project have been summarized in a software selection tool.

**OBJECTIVE**

The objective of this research project was to understand the performance of different water-resistive barriers with various vapor permeabilities in different climates and cladding applications in building wall assemblies. The sensitivity to different types of water ingress (location in the wall assembly) was examined as a function of water-resistive barrier and climate.

**SCOPE**

Variations in boundary conditions included climatic conditions (seven climatic locations), cladding type (brick, adhered manufactured stone veneer, cement-board, three-coat stucco), and type of WRB (low versus high vapor permeability) deployed.

The research approach was structured into several phases: In the first phase the water vapor permeability of different water-resistive barriers were determined as per ASTM E96-00. Subsequently a subassembly laboratory test was designed to simulate performance of a small component of a wall system during operation under controlled conditions to predict the performance of large-scale assemblies and to validate the performance simulation tool. A variation of the hygrothermal loads was performed to allow gapping between perfectly built wall assemblies and walls with realistic imperfections (workmanship issues). A number of parameters were varied to understand the sensitivity of the results to the different types of substrate, cladding, and climatic locations. In the next phase simulations were carried out with a hygrothermal computer model (WUFI 5, Karagiozis et al. 2001). The sheathing moisture content, temperature, and relative humidities were plotted against time for comparison and analysis, and presented as an index of moisture performance. In the final phase the results were embedded into a software selection tool, allowing an architect to select a specific climate zone, cladding type, water-resistive barrier with a particular perm rating, and wall orientation. Results are being presented as a function of moisture performance index (mold index).

**WATER VAPOR PERMEANCE TESTING**

Material property and subassembly tests were performed to support and strengthen the computer simulations. Table 1 shows a summary of the water-resistive barriers that were tested and their dry cup and wet cup vapor permeance values determined using ASTM E96-00 Method A and Method B (Straube et al. 2010). The test dishes were sealed with aluminum tape to ensure that the only vapor movement

observed was through the test specimen. The standard requires a minimum sample size of 3000 mm<sup>2</sup>. Samples of 16,200 mm<sup>2</sup> were used to ensure that the test results are not influenced by local variations in vapor permeance of the sample. The temperature was controlled to 23°C as specified for Method B. The relative humidity was kept constant at 50%. Further details of this part of the laboratory testing are described in Straube et al. (2010).

The wet cup (Method B) testing did result in higher average permeance values than the dry cup (Method A) testing, as anticipated. The greatest increase in vapor permeance occurred with the WRB B water-resistive barrier which nearly doubled in vapor permeance between the dry cup and wet cup tests. The wet cup vapor permeance test is more appropriate for determining the drying performance of walls as the cladding in many climates is more often between 50% and 100% relative humidity (wet cup conditions) than between 0% and 50% relative humidity.

**SUBASSEMBLY TESTING**

Testing the vapor permeance according to ASTM E96 demonstrates how the water-resistive barrier performs as an individual material, but it is also important to understand how the water-resistive barrier performs in combination with OSB or exterior gypsum sheathing, which more closely simulates a wall assembly. A subassembly laboratory study was undertaken to more clearly understand the drying ability of water-resistive barriers in combination with OSB or exterior grade gypsum sheathing. The subsystem testing was designed to simulate performance of a small component of a wall system during operation under controlled conditions to predict the performance of large-scale assemblies, and to validate the performance simulation model.

Two different types of polymeric, vapor permeable water-resistive barriers and #15 asphalt impregnated building paper were tested in the subassembly test. Twenty-seven subassembly test samples were made using three different water-resistive barriers installed on either OSB or exterior grade gypsum sheathing as shown in the testing matrix in Table 2. The differences between interior and exterior wetting are shown in Figure 1.

**Table 1. Summary of Vapor Permeance as per ASTM E96 (Dry Cup Versus Wet Cup Method)**

Water-Resistive Barrier	Method A	Method B
	Dry Cup, ng/Pa·m <sup>2</sup> ·s	Wet Cup, ng/Pa·m <sup>2</sup> ·s
WRB A	12,284 (214 perms)	13,812 (241 perms)
WRB B	804 (14 perms)	1597 (28 perms)
WRB C	3444 (60 perms)	3737 (65 perms)

Square samples measuring 330 × 330 mm (13 × 13 in.) were cut from sheets of OSB and exterior grade gypsum sheathing. The edges of the samples were wrapped with foil tape to create a 305 × 305 mm (12 × 12 in.) active test area.

Four layers of moisture storage media were installed between the sheathing and the water-resistive barrier to simulate exterior wetting or installed on the opposite side of the sheathing from the water-resistive barrier to simulate wetting on the interior, in the stud cavity as shown in the schematic in Figure 1. A 0.125 in. ID tube was installed to provide water to the moisture storage media.

Three layers of 6 mil poly were installed on the interior surface of the sheathing and sealed with aluminum foil tape to the edges of the sample. For interior wetting, the water storage media was visible through the poly to inspect the storage media for saturation.

Figures 2 and 3 show the exterior and interior surfaces of a subassembly testing sample. Figure 3 shows the wetting storage media on the interior surface through the multiple layers of polyethylene sheet.

**Table 2. Testing Matrix—Number of Subassembly Samples of Each Construction**

	OSB—Wetting		Gypsum Sheathing—Wetting	
	Interior	Exterior	Interior	Exterior
WRB A	4	1	3	1
WRB B	4	1	3	1
Building Paper	4	1	3	1

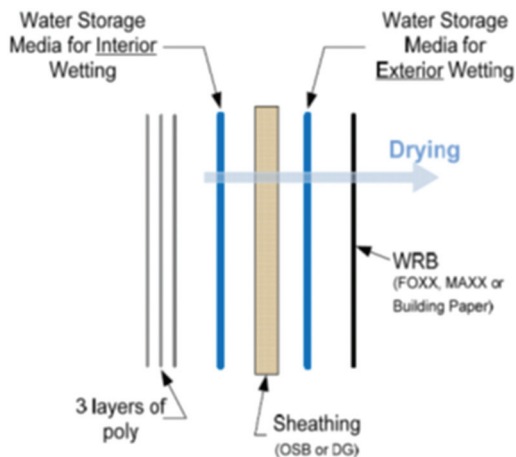


**Figure 1** Subassembly testing sample schematic.

**Procedure**

The test for each sample began by adding 100 mL (5 doses of 20 mL) by syringe to the water storage media. Each dose of water was injected over approximately 10 seconds followed by 20 seconds of wait time for water to redistribute into water storage media before adding more water. The samples were held at a constant angle for all water injections.

The samples were weighed before and after any water was added to determine the actual mass of water added by syringe. Each subsequent day, the sample was weighed to



**Figure 2** Exterior surface of subassembly test sample with exterior wetting.



**Figure 3** Interior surface of subassembly test sample with interior wetting.

determine the mass of water lost, and the same amount of water lost was added. The total mass lost and water added were graphed in Figure 4 to show the rates of both wetting and drying. If the two rates (line slopes) for wetting and drying were similar, the sample was determined to be at equilibrium and an effective permeance could be calculated.

If no water had been lost from the previous day, 20 more mL of water was added each subsequent day until “ponding” of water was observed in the water storage media through the polyethylene. This occurred when the storage media was saturated and water was not being absorbed into the substrate quickly enough.

Once the rates of wetting and drying were calculated, repeatability was determined by increasing the amount of water injected into the water storage media for two subsequent days at a rate of twice the daily loss. This dosage was increased to determine if the effective system permeance would change when a higher volume of water was added to the sample. Following the two days of increased loading, only the amount of water lost was added back to the sample.

### Boundary Conditions

The testing was conducted in a constant climate room (CCR) where the RH and temperature can be tightly controlled. The climate controls for the room were set at 23°C ( $\pm 1^\circ\text{C}$ ) and 50% rh ( $\pm 2\%$ ).

To determine the vapor pressure gradient it was assumed that the relative humidity in the sample during the testing and continuous daily wetting of the water storage media was 100%. These subassembly tests help simulate real wetting conditions, but in wall systems there are usually temperature gradients across a wall that will affect the drying rate. These tests were run with no temperature gradient across the subassembly system, which is the worst-

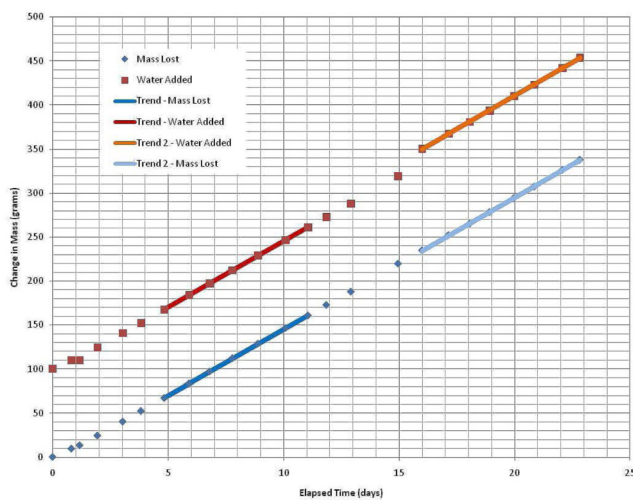


**Figure 4** Sample data set from laboratory testing (Straube et al. 2010).

case scenario for drying performance. If a temperature gradient was added, the drying rates would increase, but the ratio of drying amounts would remain the same.

### Results

**Water-Resistive Barrier A.** The dry cup vapor permeance of the WRB A water-resistive barrier according to ASTM E96, Method A is 214 perms ( $12,284 \text{ ng/Pa}\cdot\text{s}\cdot\text{m}^2$ ), and the wet cup vapor permeance according to ASTM E96, Method B is 241 perms ( $13,812 \text{ ng/Pa}\cdot\text{s}\cdot\text{m}^2$ ). This was the highest vapor permeance water-resistive barrier in the subassembly testing.

- OSB substrate: OSB has a vapor permeance of approximately 1 to 2 US perms ( $57 \text{ to } 115 \text{ ng/Pa}\cdot\text{s}\cdot\text{m}^2$ ), although the vapor permeance will change with RH as well as age of the OSB.

Figure 5 shows a typical data set from samples of OSB with interior wetting. Very little mass was lost over the duration of the test, and the water storage media became saturated with water and unable to store more. At the beginning of the test, the OSB substrate adsorbed moisture from the constant climate room that was at 50% relative humidity and 23°C and gained mass, resulting in negative mass lost on the graph, until equilibrium was reached.

The average mass lost for all OSB samples with interior wetting and WRB A was 1.4 grams per day, which is an effective sample vapor permeance of 2.2 US perms ( $126 \text{ ng/Pa}\cdot\text{s}\cdot\text{m}^2$ ).

Simulating an exterior wetting with the water storage media between the OSB and WRB A resulted in a loss of 40.6 g/day or effective sample permeance of 89 US perms ( $5107 \text{ ng/Pa}\cdot\text{s}\cdot\text{m}^2$ ).

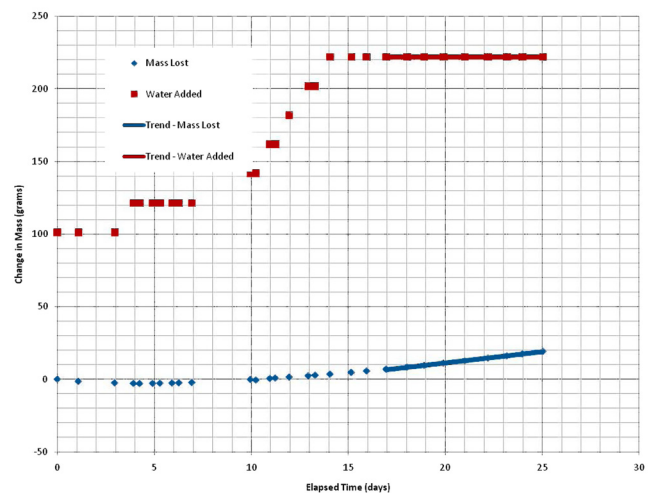


**Figure 5** Data for interior OSB wetting with WRB A (Straube et al. 2010).

- Exterior grade gypsum substrate: Moisture from interior wetting of exterior grade gypsum sheathing was able to dry much more quickly than the OSB case. The vapor permeance of the exterior grade gypsum product used in the test is 23 perms (1300 ng/Pa·s·m<sup>2</sup>), which is a value reported by the manufacturer. The average mass lost for all samples was 37.1 g/day. The effective sample permeance for wetting on the interior of the exterior grade gypsum sheathing with WRB A is 56 perms (3240 ng/Pa·s·m<sup>2</sup>).

Exterior wetting of the exterior grade gypsum sheathing was approximately the same as the exterior wetting of OSB, resulting in a daily mass loss of 52.2 g, and an effective sample vapor permeance of 92 US perms (5317 ng/Pa·s·m<sup>2</sup>).

The interior wetting of the exterior grade gypsum subassembly with WRB A dried more slowly than the exterior wetting of both OSB and exterior grade gypsum sheathing, indicating that with the higher vapor permeance WRB A, the exterior grade gypsum sheathing may limit vapor diffusion drying. WRB A is approximately ten times more vapor permeable than exterior grade gypsum sheathing.

**Water-Resistive Barrier B.** The dry cup vapor permeance of WRB B according to ASTM E96 Method A is 14 US perms (804 ng/Pa·s·m<sup>2</sup>) and the wet cup vapor permeance according to ASTM E96 Method B is 28 US perms (1597 ng/Pa·s·m<sup>2</sup>). WRB B has a much greater vapor permeance than OSB which is 1 to 2 perms (57 to 115 ng/Pa·s·m<sup>2</sup>), and WRB B has approximately the same vapor permeance as exterior grade gypsum sheathing which is 23 perms (1300 ng/Pa·s·m<sup>2</sup>) when WRB B is in a high RH environment (simulated by Method B wet cup ASTM E96).

- OSB substrate: Subassembly testing of OSB and WRB B performed similarly to the WRB A. The vapor permeance of the OSB was the controlling force in drying from interior wetting. The mass lost during interior wetting was 1.7 g/day, which is an effective sample permeance of 1.7 perms (96 ng/Pa·s·m<sup>2</sup>).

Exterior wetting of the OSB with WRB B resulted in 16.1 g/day or an effective sample permeance of 24.8 perms (1423 ng/Pa·s·m<sup>2</sup>).

- Exterior grade gypsum substrate: Interior wetting of the exterior grade gypsum sheathing with WRB B resulted in a mass loss of 15.0 g/day, which is an effective sample permeance of 23 perms (1327 ng/Pa·s·m<sup>2</sup>).

Exterior wetting between the exterior grade gypsum substrate and WRB B resulted in a mass loss of 16.1 g/day and an effective sample permeance of 24.8 perms (1423 ng/Pa·s·m<sup>2</sup>).

The effective permeance for the exterior and interior wetting of exterior grade gypsum sheathing, and the exterior wetting of OSB with WRB B all have similar mass loss and effective sample vapor permeances. This means that in the subassembly test of interior wetting on exterior

grade gypsum sheathing, the limiting factor for drying was the WRB B, not the exterior grade gypsum sheathing. The vapor permeances in all cases were lower with WRB B than with WRB A, but in the case of interior wetting of OSB, the difference is insignificant.

**Building Paper (#15 Felt).** The range of properties for building paper can vary significantly. According to *ASHRAE Handbook—Fundamentals* the vapor permeance of different thickness #15 felt ranges from 0.5 to 40 perms (28 to 2300 ng/Pa·s·m<sup>2</sup>) over a range of relative humidities. For these tests, the relative humidities during wetting events were quite high, so the permeances were likely at the higher end of the range at that time. As the subassemblies dried out the permeance would drop again to a low range depending on the relative humidities.

- OSB substrate: Interior wetting of OSB with building paper resulted in an average mass loss of 0.5 g/day or an effective sample permeance of 0.8 perms (45 ng/Pa·s·m<sup>2</sup>). This is the slowest drying of all interior OSB wetting.

Exterior wetting of the OSB with building paper resulted in a mass loss of 12.0 g/day or an effective sample permeance of 18.6 perms (1070 ng/Pa·s·m<sup>2</sup>). This is the lowest of all exterior wetting on OSB subassembly tests.

- Exterior grade gypsum substrate: Interior wetting of the exterior grade gypsum sheathing with building paper resulted in a mass loss of 9.3g/day, which is an effective sample permeance of 13.8 perms (794 ng/Pa·s·m<sup>2</sup>). Exterior wetting between the exterior grade gypsum sheathing and building paper resulted in a mass loss of 10.7 g/day and an effective sample permeance of 15.8 perms (908 ng/Pa·s·m<sup>2</sup>).

## Summary Subassembly Testing

Table 3 shows a summary of the subassembly testing results and the effective sample vapor permeances.

The following conclusions can be drawn from Table 3:

- If water were to enter on the interior of the OSB, it would dry twice as quickly with WRB B as with building paper and three times as quickly with WRB A as with building paper, although the rate of drying is quite slow since the permeance in all cases is controlled by the absorptivity and vapor permeance of the OSB.
- If water were to enter on the interior of exterior grade gypsum sheathing, it would dry 1.5 times as quickly with WRB B instead of building paper, and would dry 2.5 times as quickly with WRB A as with building paper.
- If water were on the exterior of the OSB sheathing between the sheathing and the water-resistive barrier, it would dry 1.3 times more quickly with WRB B than with building paper, and 3.3 times more quickly with WRB A than with building paper.

**Table 3. Summary of Subassembly Test Results and Effective Sample Permeances**

	Mass Loss, g/day	Effective Sample Permeance	
		US Perms	ng/Pa·s· m <sup>2</sup>
<b>WRB A</b>			
Interior wetting on OSB	1.4	2.2	126
Exterior wetting on OSB	40.6	89	5108
Interior wetting on gypsum sheathing	37.1	56.4	3240
Exterior wetting on gypsum sheathing	52.2	92.6	5317
<b>WRB B</b>			
Interior wetting on OSB	1.1	1.7	96
Exterior wetting on OSB	16.1	24.8	1423
Interior wetting on gypsum sheathing	15	23.1	1327
Exterior wetting on gypsum sheathing	16.1	24.8	1423
<b>Building Paper</b>			
Interior wetting on OSB	0.5	0.8	45
Exterior wetting on OSB	12	18.6	1070
Interior wetting on gypsum sheathing	9.3	13.8	794
Exterior wetting on gypsum sheathing	10.7	15.8	908

If water were on the exterior of the exterior grade gypsum sheathing between the sheathing and the water-resistive barrier, the water would dry 1.5 times more quickly with WRB B than with building paper, and almost 5 times more quickly with WRB A than with building paper.

These tests were conducted without a temperature gradient across the subassembly sample. Using a temperature gradient would increase the vapor pressure equally for all samples, and should increase the drying rate equally.

In all cases, the effective permeance of the samples with WRB A had a higher effective vapor permeance than the similar tests with WRB B, and the WRB B samples had a higher effective vapor permeance than similar tests with building paper.

In all cases of interior wetting of the OSB, with no temperature gradient, the drying was very slow and controlled by the OSB sheathing. The type of water-resistive barrier did not significantly affect the drying rate of the OSB.

Comparing the exterior wetting of OSB and exterior grade gypsum sheathing with WRB B, the resulting effective vapor permeance is very close to the ASTM E96 wet cup value of 28 perms (1597 ng/Pa·s·m<sup>2</sup>) determined in phase one

of this study. Exterior wetting beneath the WRB A resulted in effective vapor permeances of approximately 1/3 of the ASTM E96 wet cup value. WRB A has a high vapor permeance and may not have been maintaining 100% rh between the sheathing and the water-resistive barrier.

### SIMULATIONS WITH HYGROTHERMAL MODEL

The thermal and hygric behavior of building enclosure components are closely interrelated and therefore have to be investigated together. Permanently increased moisture content in a building enclosure component may result in moisture damages and mold growth. Increased moisture content in building components favors heat losses, and thermal conditions affect moisture transport.

To investigate how the water-vapor permeability of a water-resistive barrier affects the performance of a building enclosure under various climatic conditions and in conjunction with different sheathing materials and cladding materials, hygrothermal simulations were performed with WUFI 5. This software model allows the one-dimensional investigation of the hygrothermal performance of building components including effects like built in moisture, driving rain, solar radiation, long-wave emission, capillary transport, and summer condensation (Künzel and Karagiozis, ASTM Manual 40 2001).

The following climatic locations were chosen for the hygrothermal simulations (climate zone references as per the International Energy Conservation Code zoning):

- Miami, FL (Climate Zone 1)
- New Orleans, LA (Climate Zone 2)
- Atlanta, GA (Climate Zone 3)
- San Francisco, CA (Climate Zone 3)
- Baltimore, Maryland (Climate Zone 4)
- Portland, OR (Climate Zone 4)
- Seattle, WA (Climate Zone 4)
- Chicago, IL (Climate Zone 5)
- Minneapolis, Minnesota (Climate Zone 6)
- Fairbanks, Alaska (Climate Zone 7)

Two different exterior sheathing materials were considered for the hygrothermal simulations: Oriented strand board (OSB) and exterior grade gypsum board.

The following cladding materials were investigated:

- Brick
- Adhered manufactured stone veneer
- Cementitious stucco
- Cementitious siding

Six different water-resistive barrier scenarios were investigated:

- Building paper
- Low-perm membrane (1 perm)
- WRB A

- WRB B
- WRB C
- Combination of WRB C with ventilated rainscreen membrane (Product D)

In regards to the inner wall construction IRC code requirements were deployed, (e.g., a vapor retarder on the warm side of the insulation was only used where required by building code). The building paper and the low-perm membrane case were used for comparison. The last case (combination of WRB C with ventilated rainscreen D) comprised a highly water-vapor permeable water-resistive barrier with an impermeable, three-dimensional rainscreen HDPE membrane (dimple sheet) which was ventilated on the front and backside. This scenario was chosen to investigate the beneficial effect of combining drying potential for any moisture within the wall cavity (via vapor diffusion through the permeable water-resistive barrier into the ventilated cavity outside) and an impermeable layer outboard of the ventilated airspace in order to prevent inward moisture movement from absorptive cladding due to solar drive. The beneficial effect of a ventilated vapor impermeable rainscreen product has been evaluated and discussed in detail by Straube et al (2009) and by Jablonka et al. (2010).

The key properties for water-resistive barriers that were measured earlier on in the project were used in the analysis. The heat (conduction) and moisture transport (vapor diffusion and capillary conduction) were deployed in the simulations in one-hour time steps. Hourly indoor and outdoor climatic conditions as per ASHRAE Standard 160-2009 were used and the assumption was applied that 1% of the precipitation water that hits the cladding would leak through or enter behind the cladding. Additional analysis was performed where 0.75% water penetration took place between the water-resistive barrier and sheathing board, and 0.5% of water penetration between the sheathing board and insulation were also included into the parametric. Analysis was performed in one-hour steps for a two-year period for the selected wall enclosure systems. The interior conditions were calculated from the exterior weather file used in the hygrothermal simulation by applying the intermediate method from ASHRAE Standard 160-2009.

Material property inputs were taken from the WUFI North American database with the exception of the adhered manufactured stone veneer where measured data was used. The WUFI database for North America includes the data from NRC (Kumaran 2001).

### Connection of Model and Subsystem Testing

As with all modeling activities, it is important to capture the subsystem effects. When these subsystem effects are properly captured, the accuracy of the predictions are expected to be higher. Prior to the execution of the hygrothermal analysis, the basic properties of the water-resistive barriers were measured (Straube et al. 2010). Then a series of subsystem tests were performed as described in the previous sections. The 1D hygrothermal model (WUFI 5) was used to validate the drying performance of the various experimental results. Good agreement was found between the model predictions and the measured drying rates for the various laboratory subsystems tested. The validation provided the necessary confidence in the results to engage in the comprehensive hygrothermal parametric analysis.

For the simulation cases that included the ventilated rainscreen D, two air cavities were included into the WUFI 5 model. The air exchange rates within the two air cavities were calculated based on the procedure developed within ASHRAE TRP 1091 (Burnett et al. 2004) which was also detailed in *Journal of ASTM International* by Karagiozis and Kuenzel (2009). The flow equations with the entrance and exit pressure drops were used, as well as the flow resistance along the length of the ventilated rainscreen membrane (product D). The effect of stack pressures, wind pressures, and moisture concentration gradients are combined to produce a net force for driving airflow in each of the two cavities that the ventilated rainscreen D creates. These mass flows were converted into cavity air changes per hour (Karagiozis and Kuenzel 2009) and allowed to calculate the dynamic impact of exterior and interior boundary conditions. Input files were created for the hygrothermal analysis using WUFI. The WUFI model has been extensively validated for many different cladding cavity configurations and has shown excellent agreement with measured field data.

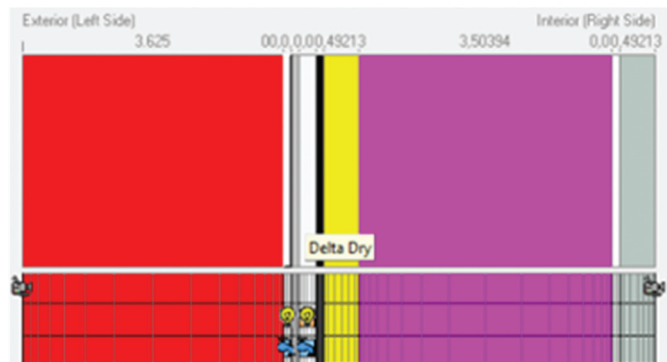


**Figure 6** Ventiladed rainscreen D, configuration within wall assembly.

Three surfaces were selected as the critical layers for detailed analysis: The exterior surface of the exterior sheathing board (P1), the interior surface of the exterior sheathing board (P2), and the interior side of the insulation layer in the wall cavity (P3). Selection points both on the interior and exterior side of the wall cavity ensured that the climatic effects were captured in the performance analysis.

The maximum mold growth index for each point was investigated. The mold growth index, as described in depth by Viitanen (Viitanen 2010) makes it possible to analyse the critical conditions needed for the start of mold growth and to measure the progress of mold growth.

First, all points were checked against a reference value. The average of the maximum mold growth index of these three points was calculated, and this value was then used as a performance indicator for ranking. The lowest value has the highest ranking, representing the best wall performance in regards to moisture management.

## SOFTWARE SELECTION TOOL

Wall assemblies with various cladding types in different climates demand the proper selection of water-resistive barriers for optimal performance. The results of the measurements and hygrothermal simulations with WUFI 5 described in this paper were summarized in a software tool that helps the designer simply and effortlessly choose the most suitable water-resistive barrier for a particular wall assembly configuration. Furthermore, it provides a design recommendation for optimal wall performance based on a performance ranking by water-resistive barrier type. A damage function is used for guidance to provide insight on performance of these different water-resistive barriers.

The software tool allows for a step-by-step selection process as shown in Figure 7.

The user gets prompted to select the location from a list or map. A total number of 13 locations are available for selection by the user. These locations were carefully selected in

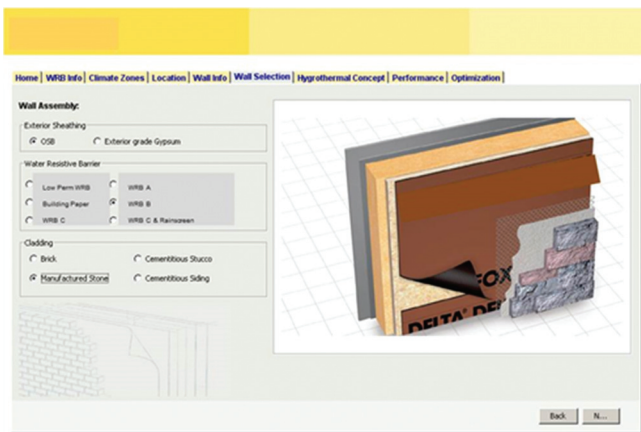


**Figure 7** Software tool for simple selection of most suitable water-resistive barrier.

order to cover all climatic zones of the US; the user would choose the location that would be closest to the location of interest within the same climate zone. In the next step the user gets prompted to choose the type of exterior sheathing (OSB or exterior grade gypsum board). Furthermore the user can choose from one of six options for water-resistive barrier with a wide range of water vapor permeability. The last step in the selection process allows the user to decide between four different cladding options: Brick, adhered manufactured stone veneer, cementitious stucco, and cementitious cladding.

The performance results for the selected wall assembly for that particular climatic location are then presented in a summary screen as shown in Figure 8.

The summary screen provides three gauges with a range from 1 to 6. In this way the designer is provided with a simple overview of how well a particular wall assembly would function under the chosen conditions.

The first gauge on the left provides the maximum mold growth index for the assumed best case scenario that 1% of the precipitation water that hits the façade will leak through the cladding but remain on the outside of the water-resistive barrier. The second gauge in the middle provides the maximum mold growth index for the assumed case that 0.75% of that water enters between the water-resistive barrier and the sheathing board. The third gauge on the right presents the maximum mold growth index for the assumed case that 0.5% of that water enters into the wall cavity (backside of the exterior sheathing material). By presenting all three gauges in one view the designer gets a quick impression how well a wall assembly would perform under optimal versus suboptimal (more realistic) conditions (e.g., missing flashing, penetrations in water-resistive barrier).

If desired, the designer can pull up detailed graphs for temperature, relative humidity, and moisture content for each of the three scenarios. The graph in Figure 9 shows a typical example for temperatures measured in the three sensor locations P1, P2, and P3 for the simulated two-year period.

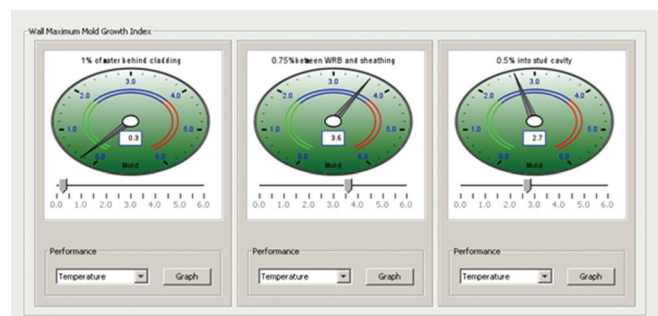


**Figure 8** Summary screen for wall performance under selected conditions.

For simplicity a performance overview is provided to the designer as shown in Figure 10.

The performance overview chart shows the six different water-resistive barrier scenarios that were analyzed. Lowest mold growth index (optimum hygrothermal performance) is achieved in the center of the diagram. The further the red line moves to the outside of the diagram, the more mold growth has to be expected under the chosen circumstances. The list below the diagram shown in Figure 10 provides a performance ranking of the different water-resistive barrier scenarios for that particular climate zone and the chosen sheathing board and cladding type.

It is apparent that the vapor permeability of the water-resistive barrier has an influence on the average mold growth index, as it affects the drying of interior moisture via diffusion.

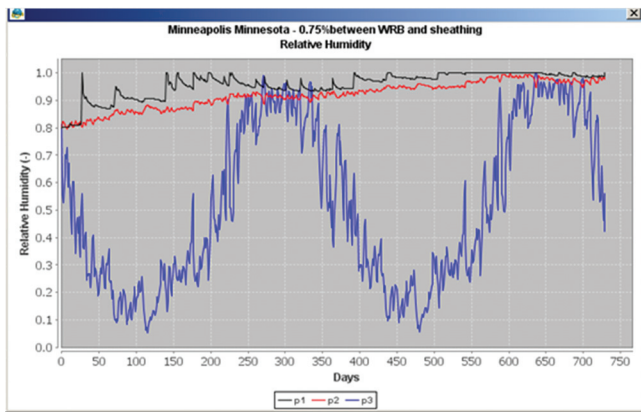


Figure 9 Relative Humidity predicted over 2 years in locations P1, P2, and P3 for selected conditions.

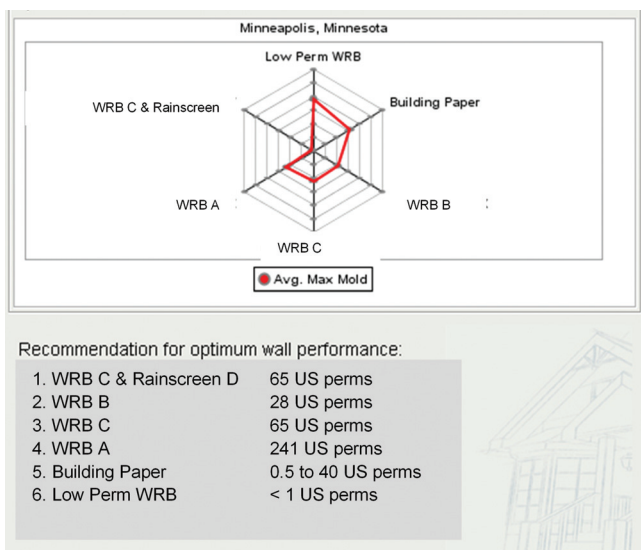


Figure 10 Performance overview and performance based ranking for various WRB options: Smaller values (center of diagram) indicate better performance.

Figure 11 and Figure 12 show the average mold growth index for Chicago for adhered manufactured stone veneer and cementitious siding with OSB as exterior sheathing material.

Figures 13 and 14 show the relative humidity in the three different sensor locations for the same location and cladding materials (1% of precipitation leaked behind cladding).

Figure 13 shows that in the Chicago climate, the use of a highly vapor permeable water-resistive barrier used behind adhered manufactured stone veneer would lead to elevated

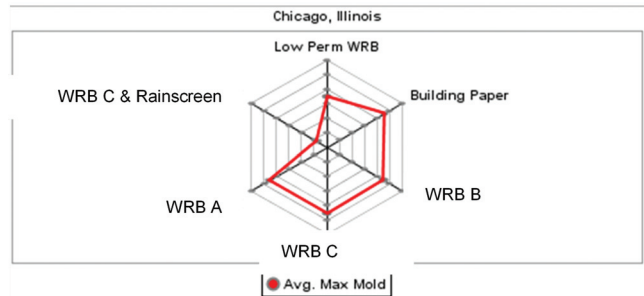


Figure 11 Average mold growth index Chicago, adhered manufactured stone veneer, OSB as exterior sheathing.

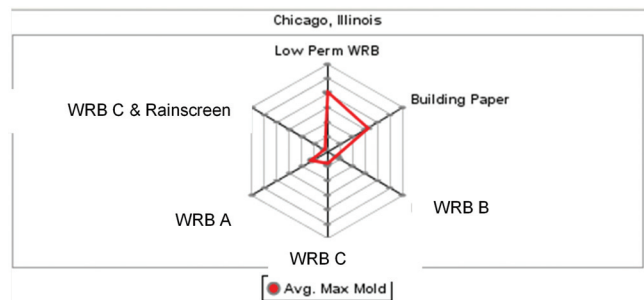


Figure 12 Average mold growth index Chicago, cementitious siding, OSB as exterior sheathing.

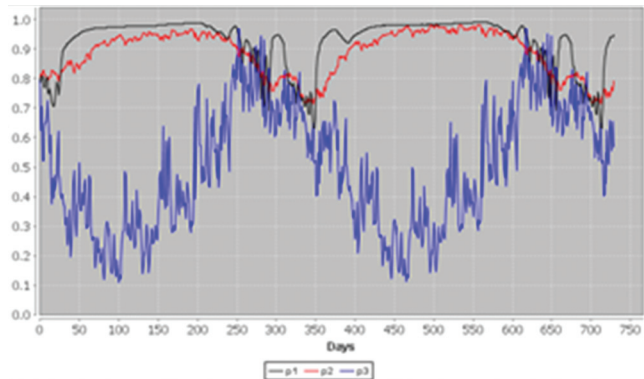
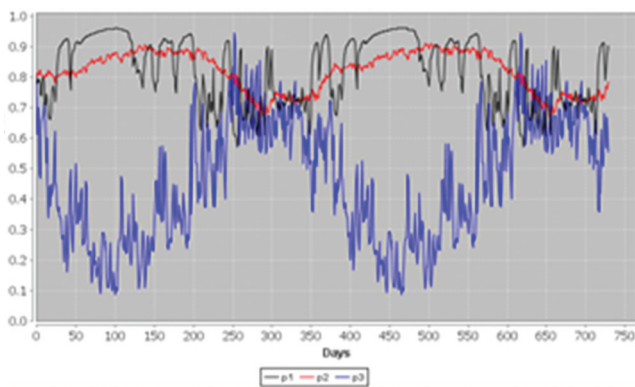


Figure 13 Relative humidity Chicago, adhered manufactured stone veneer, OSB and WRB C (65 US perms).

levels of relative humidity for long time periods per year (between 90% and 100% rh). The same water-resistive barrier used behind cementitious siding would lead to significantly lower RH values for most of the year (between 70% and 90%). The elevated levels can be explained with solar moisture drive from highly absorptive claddings into the wall cavity. A highly vapor-permeable membrane would allow moisture from the inside of the cavity to easily diffuse to the outside, but in case of reverse vapor pressure differential moisture can also easily diffuse inwards and elevate the moisture levels inside the wall assembly.

The reverse moisture flow can be prevented by using a ventilated, vapor impermeable rainscreen outboard of a highly vapor permeable water-resistive barrier as shown in Figures 15 and 16 (1% of precipitation leaked behind cladding).

The graphs show that by utilizing a highly vapor permeable water-resistive barrier in conjunction with an imperme-



**Figure 14** Relative humidity Chicago, cementitious siding, OSB and WRB C (65 US perms).

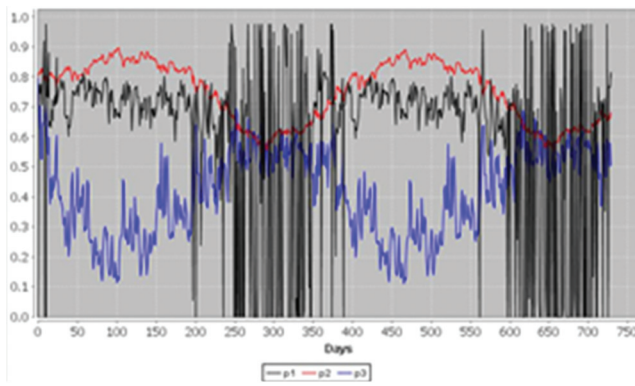


**Figure 15** Relative humidity Chicago, adhered manufactured stone veneer, OSB, and WRB C (65 perms) with rainscreen.

able rainscreen product on the outside, the relative humidity levels drop noticeably.

Similar results can be seen for other climate zones. Optimum wall performance in any climate zone can generally be achieved by combining a highly vapor permeable water-resistive barrier with an impermeable, ventilated rainscreen material. This combination allows for quick drying of moisture from within the wall assembly to the outside, while moisture from the outside (i.e., stored in absorptive cladding material like adhered manufactured veneer) cannot migrate inward.

## CONCLUSIONS

This paper evaluates the impact of various water-resistive barriers with a large range of vapor permeability on the hygrothermal performance of different wall assemblies. A simple-to-use tool has been developed after it was validated with laboratory results.

The results from this tool enable designers to select products with the most suitable vapor permeability for a particular geographical location under specific construction conditions. Variations in boundary conditions included climatic conditions (from seven climatic zones), cladding type (three-coat stucco, manufactured stone, cement board, brick), and type of water-resistive barrier (low versus high vapor permeability) deployed. The results for the performance of the wall systems are presented in form of a mold index. The approach presented includes three possible wetting locations and examines the best drying potential as a function of a range of vapor permeability of the water-resistive barriers.

## REFERENCES

- ANSI/ASHRAE Standard 160-2009, *Criteria for Moisture-Control Design Analysis in Buildings*, ASHRAE.
- ASHRAE. *ASHRAE Handbook—Fundamentals* (2009): Heat, Air and Moisture Control in Building Assemblies—Material Properties, Chapter 26.
- ASTM E96-00, *Standard Test Methods for Water Vapor Transmission of Materials*.

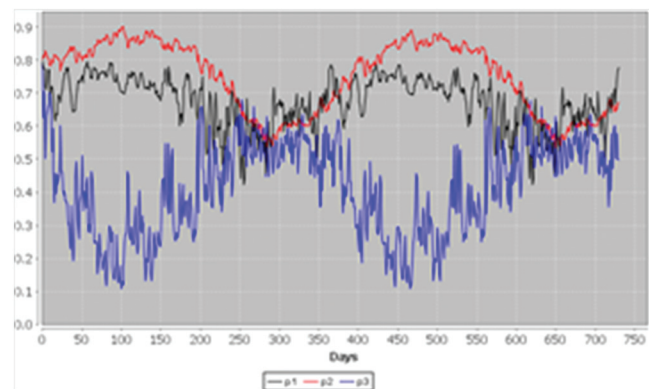


**Figure 16** Relative humidity Chicago, cementitious siding, OSB and WRB C (65 perms) with rainscreen.

- Burnett, E., Straube, J., and Karagiozis, A. (2004): Synthesis Report and Guidelines, ASHRAE TRP-1091, Report No. 12.
- Carmeliet, J., Karagiozis, A., and Derome, D. (2007): Cyclic Temperature-Gradient-Driven Moisture Transport in Walls with Wetted Masonry Cladding, Thermal Performance of the Exterior Envelopes of Buildings X, *Proceedings of ASHRAE THERM X*, Clearwater, FL, December 2007.
- Jablonka, M. (2011): DELTA-iSelect, an easy to use software tool to select WRBs based on durability analysis, *IEA Annex 55, Proceedings of 4th Meeting*, San Antonio, Oct. 14–16, 2011.
- Jablonka, M., Karagiozis, A., and Straube, J. (2010): Innovative Passive Ventilation Water-resistive Barriers—How do they work?, *ASHRAE Transactions* (2010, Vol. 116, Part 2).
- Karagiozis, A., and Kuenzel, H. (2001): WUFI-ORNL/IBP-A North American Hygrothermal Model, *Proceedings for the Performance of Exterior Envelopes of Whole Buildings VIII; Integration of Building Envelopes*, Clearwater, FL, December 2001, pp. 547–554.
- Karagiozis, A., and Kuenzel, H. (2009): The Effect of Air Cavity Convection on the Wetting and Drying Behavior of Wood-Frame Walls Using a Multi-Physics Approach, *Journal of ASTM International*, Vol. 6, No. 10, Paper ID JAI101455.
- Künzel, H.M., Karagiozis, A.N. and Holm, A. (2001): *Moisture Analysis and Condensation Control in Building Envelopes*, Manual 40, West Conshohocken, Pa., American Society for Testing and Materials, Chapter 9.
- Kumaran, K. (2001): Hygrothermal Material Properties, ASHRAE TRP-1018.
- Straube, J., Schumacher, C., Smegal, J., and Jablonka, M. (2009): Adhered Veneers and Inward Vapor Drives: Significance, Problems and Solutions, *Journal of Building Enclosure Design*, Summer 2009.
- Straube, J., Smegal, J., and Schumacher, C. (2010): Water-resistive barrier laboratory testing – ASTM E96, Building Science Consulting Inc., Lab report, February 16, 2010.
- Straube, J., Smegal, J., Schumacher, C. (2010a): Water-resistive barrier sub-assembly laboratory testing, Building Science Consulting Inc., Lab report, March 24, 2010.
- Viitanen, H. (2010): Moisture conditions and biodeterioration risk of building materials and structure, *Journal of Building Physics* January 2010 vol. 33 no. 3 201–224.